Journal of Fluids and Structures (2000) **14,** 691–696
doi:10.1006/jfls.2000.0293 available online at http://www.idealibrary.com on IDEAL®

FLOW PAST A 2-D BACKWARD-FACING STEP WITH AN OSCILLATING WALL

F. Huteau, T. Lee and D. Mateescu

Department of Mechanical Engineering, McGill University
Montreal, Quebec, Canada H3A 2K6

(Received 16 April 1999, and in final form 15 February 2000)

The spatial-temporal movements of the reattachment (x_r) and separation (x_s) points in a 2-D backward-facing step flow with a bottom wall oscillated sinusoidally at selected frequencies and amplitudes were characterized using multiple hot-film sensor arrays and smoke flow visualization methods. The results also show that both x_r and x_s moved toward (away from) the step during upward (downward) motion of the wall, and that their rate of variation or the covered distance is a strong function of the wall oscillation. The present measurements would provide a practical means for the study of unsteady separated flows, as well as for the validation of CFD modelling.

1. INTRODUCTION

The separation of the flow and its subsequent reattachment to a solid surface occurs in many industrial and aeronautical systems. The importance and complexity of such flows to engineering equipment has been stressed in many publications [e.g. see Abbott and Kline (1962), Eaton and Johnston (1981)]. However, in order to obtain a better understanding of the complex reattachment process, the separated flow behind a 2-D backward-facing step has frequently been chosen as an environment for validating new experimental measuring techniques [e.g. Goldstein *et al.* (1970), Eaton *et al.* (1979), Armaly *et al.* (1983), Driver *et al.* (1987), Grant *et al.* (1992)] and/or numerical fluid dynamics simulation codes [e.g., Gartling (1990), Mateescu *et al.* (1994)]. Recently, the locations of the reattachment and laminar separation points induced by a 2-D step under steady flow conditions were measured nonintrusively by Lee & Mateescu (1998) using multiple hot-film sensor arrays, and compared to their numerical predictions for Re ($= u_{\text{avg}}H/\nu$, where u_{avg} is the inlet average velocity based on inlet volumetric flow rate and the cross-sectional area, H is the step height, and ν is the fluid kinematic viscosity) < 1300 and an expansion ratio ER ($= H_d/H_u$, where H_u and H_d are the channel heights upstream and downstream of the step, respectively) of 2. However, only a comparatively small number of researchers have investigated the effects of the flow unsteadiness on the reattachment process in a 2-D step flow (Mullin *et al.* 1980, Westphal & Johnston 1984).

Mullin *et al.* (1980) examined the influence of the flow unsteadiness on the flow reattachment process by pulsating the flow over a step. They reported that, depending on the pulsation frequency, the recirculation vortex was shed or stationary but smaller than for steady flow. Westphal & Johnston (1984) studied the influence of adverse pressure gradient or ER on the shear-layer reattachment caused by rotating the upper wall of a 2-D step flow. They concluded that the result of altering the adverse pressure gradient by rotating the channel wall is consistent with the result where adverse pressure gradient was altered by

0889–9746/00/070691 + 06 $35.00/0

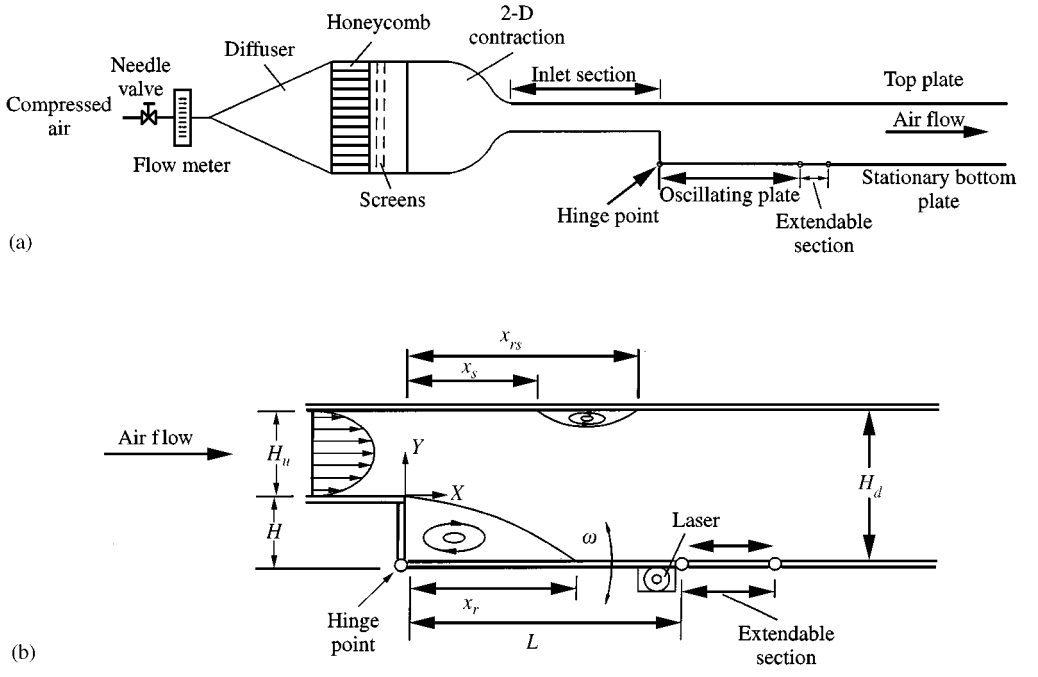

Figure 1. Schematic of (a) the experimental set-up, and (b) geometry of the flow.

changing the ER. However, detailed experimental characterization of the instantaneous locations of the reattachment and laminar separation points under the influence of the flow unsteadiness is still needed. In the present experiment, the effects of the flow unsteadiness (generated by small-amplitude forced oscillation of the wall immediately downstream of a 2-D step) on the spatial-temporal movement of these points for $\mathrm{Re} < 1200$ were examined using multiple hot-film sensor arrays and smoke flow visualization methods.

2. EXPERIMENTAL METHODS

A 2-D channel flow with a width-to-height ratio of 26·6 was used in the present experiment. It incorporated a 2-D backward-facing step with a fixed H of 1·5 cm and an ER of 2. The test-section was machined from 1·27-cm-thick sheets of Plexiglas, then fitted with instrument ports and a specially designed cam-follower oscillation mechanism (Figure 1). The origin of the coordinate system is centred at the step corner. The inlet compressed air passed through a flow control system and a section with flow straighteners and steel wool, and was afterwards guided into a smooth contraction section with a contraction ratio of 20. The inlet flow rate was kept constant by using the flow control system which consists of a pressure gauge, a precision needle valve, and a flow meter. The outlet of the contraction was connected to the inlet of the upstream channel test-section, which was 2 m in length, 40 cm in width, and 1·5 cm in height. The length of constant-area duct upstream of the step could be varied by adding or removing sections of duct. A portion of the bottom wall ($L = 40$ cm) immediately downstream of the step was oscillated sinusoidally with $\delta^* = \Delta\delta/H = \pm 0{\cdot}2 - \pm 0{\cdot}6$, where $\Delta\delta$ is the amplitude of the oscillation at the end of the oscillating plate, and $\kappa = f_0 H/u_{\mathrm{avg}} = 0{\cdot}04 - 0{\cdot}08$, where f_0 is the oscillation frequency. The instantaneous vertical position, $\delta(t)$ $(= \Delta\delta\cos\omega t)$, of the plate was recorded using

a laser-based electro-optic transducer (Hamamatsu Model S3931) through a linear position-voltage (δ-E) calibration relationship. The light beam from a miniature 0·4 mW He–Ne laser (mounted underneath and at the end of the bottom wall) was focused onto the position-sensitive detector (PSD). The spot image moves along the photosensitive surface of the detector which causes changes in the detector output voltage and thereby allows the measurement of $\delta(t)$ of the wall.

A total of 480 micro-thin (0·2 μm in thickness) multiple hot-film sensors arranged in a straight-line array were used to identify the spatial-temporal movements of the reattachment and separation points on the bottom and top walls, respectively. Each sensor consists of a 0·1-mm wide nickel film with 10 μm copper-coated nickel leads routed to provide wire attachment away from the measurement location. Sensors S_1–S_{240} (S_{241}–S_{480}) with a sensor spacing of 1·3 mm were on the bottom (top) wall with sensor S_1 (S_{241}) located at $x = 25$ mm (35 mm) downstream from the step. Groups of 16 of the 480 sensors were systematically connected to 16 constant-temperature anemometers (CTAs) to obtain both time history and spectral information at each sensor position. The overheat and offset voltages for each sensor were carefully adjusted such that each sensor was at nearly the same operating conditions. The CTA output signals were sampled at 1 kHz per channel

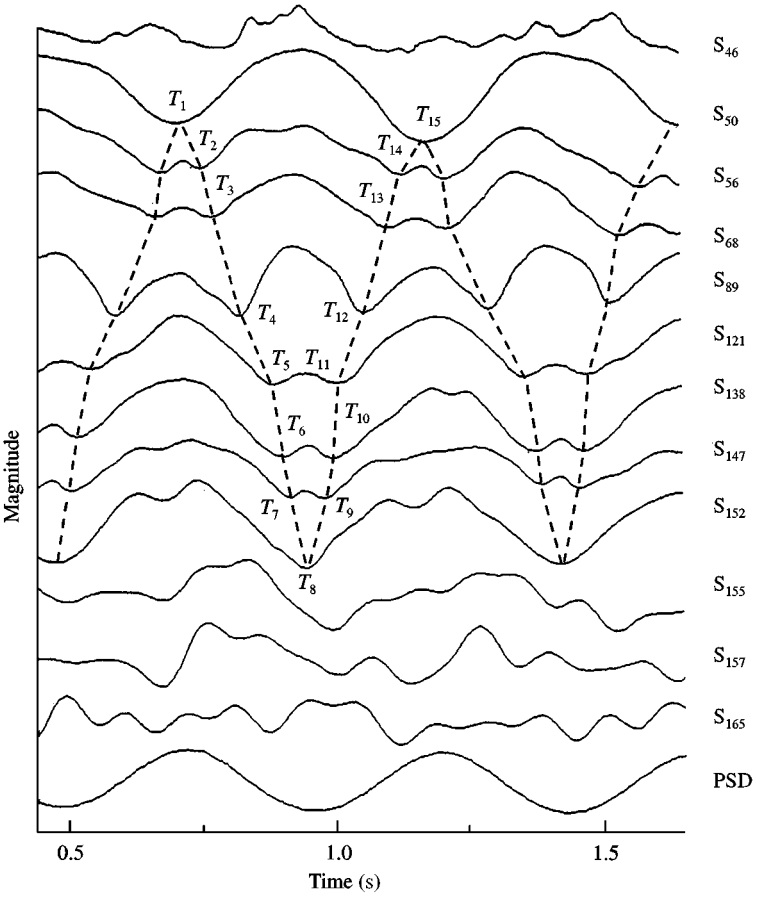

Figure 2. Typical composite plots of selected simultaneously-acquired hot-film (S_{46}–S_{165}) signals and PSD outputs for an oscillating wall with $\delta^* = \pm 0{\cdot}60$, $\kappa = 0{\cdot}04$, and Re = 745.

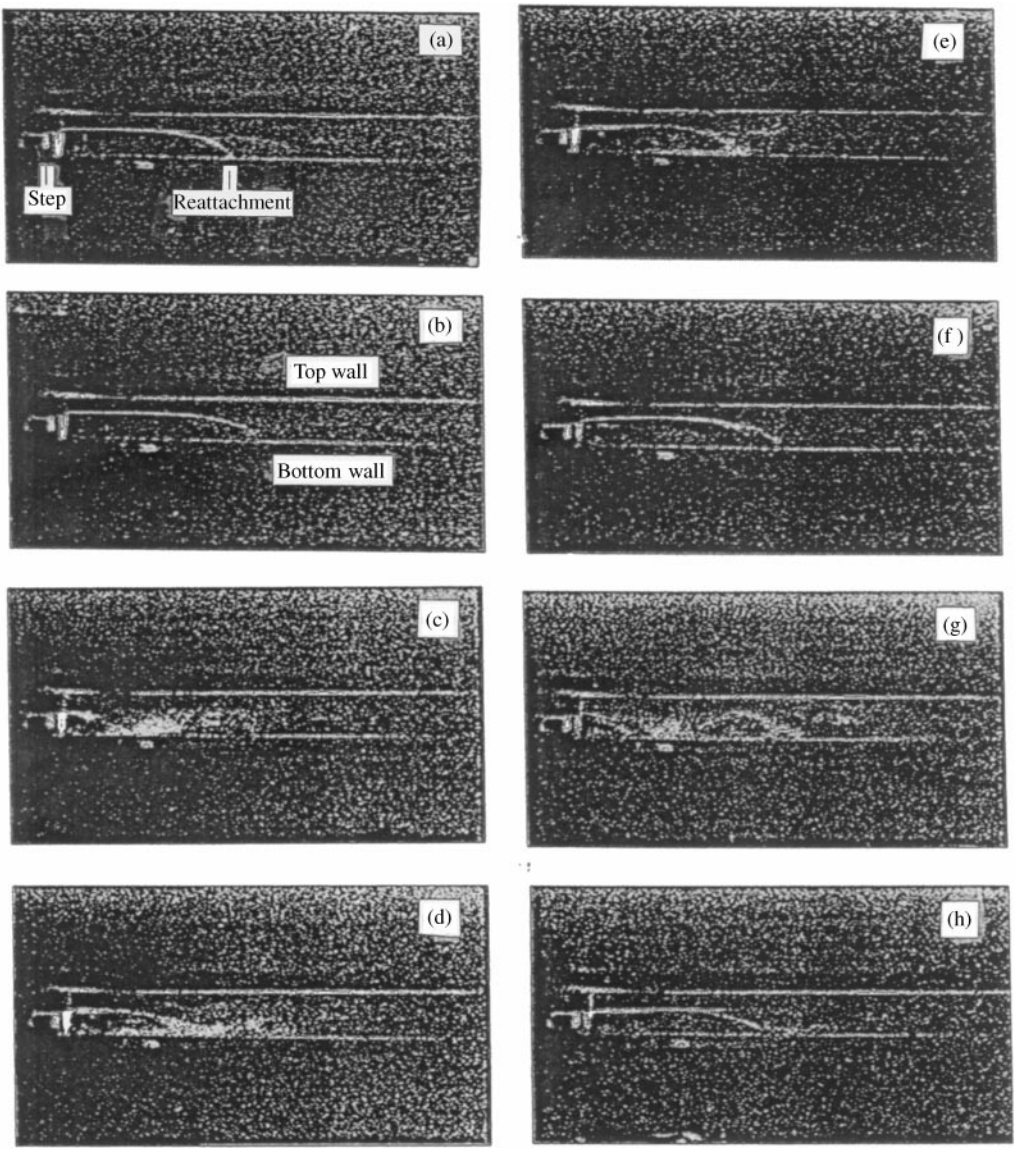

Figure 3. Smoke flow visualization results. Stationary wall: (a) $x_r^* \approx 10$, Re = 545; (b) $x_r^* \approx 11{\cdot}5$, Re = 745. Oscillating wall with $\delta^* = \pm 0{\cdot}59$, $\kappa = 0{\cdot}04$, and Re = 745: (c) $x_r^* \approx 5$ at $\tau = \pi/6$; (d) $x_r^* \approx 8$ at $\tau = \pi/3$; (e) $x_r^* \approx 10$ at $\tau = 2/3\pi$; (f) $x_r^* \approx 12{\cdot}5$ at $\tau = 5\pi/6$; (g) $x_r^* \approx 13{\cdot}5$ at $\tau = \pi$; (h) $x_r^* \approx 11{\cdot}5$ at $\tau = 7\pi/6$.

through a 586 PC with a 12-bit A/D converter board. The sensor outputs were also connected to a four-channel spectral analyzer (LeCroy model 9304) to provide on-line time history traces of the operating groups of sensors. Details of the hot-film sensor pattern and the layout of the leads, and their operations are given in Lee & Basu (1998) and Lee & Mateescu (1998).

3. RESULTS AND DISCUSSION

Figure 2 shows the typical composite plots of the time traces of selected hot-film sensors (S_{46}–S_{165}) output signals from an oscillating wall with $\delta^* = \pm 0{\cdot}6$, $\kappa = 0{\cdot}04$, and Re = 745. The numbers shown on the right side ordinate axes in this figure correspond to sensor numbers on the oscillating plate. The lowermost curve represents the variation in the PSD output voltage, which indicates the location of a reference sensor on the plate at a given instant. The y-axis represents the self-scaled voltage output level of each sensor, which allows the regions of change to be conveniently identified. The repeatability from cycle to cycle was found to be extremely good, and for clarity only about 2·5 cycles needed to be shown. Figure 2 reveals that the movement of the reattachment point x_r with time, t, under the influence of small-amplitude oscillation is clearly indicated by the travel of the minimum voltages from outputs of S_{50}–S_{149} during one cycle of oscillation. Sensor S_{50} at time instant T_1 traverses the instantaneous reattachment point first followed by sensors S_{56}–S_{152} (at T_2–T_8) during downward motion, and then followed by sensors S_{147}–S_{50} (at T_9–T_{15}) during upward motion of the wall. The hot-film measurements were also compared to the values estimated from the smoke flow visualization results (Figure 3). The smoke was generated by a smoke generator and was induced into the 2-D flow field through a 1-mm-diameter hole at the edge of the step. The flow patterns were recorded with a 60 Hz video camera (with a shutter speed of 1/500 s) as well as recorded on ASA 3200 film using a 35 mm still camera with a macro-zoom-lens.

Figures 3(c–h) show that the reattachment length $x_r^* = x_r/H$ oscillates between approximate $5 \leq x_r^* \leq 13{\cdot}5$ [compared to $x_r^* \approx 11{\cdot}5$ for a stationary wall; Figure (3b)], and that there is a presence of two recirculation regions downstream of the step which occurred approximately at the end of downward motion of the wall [Figure 3(g)]. The flow visualization results (indicated by solid symbols) are also compared with the hot-film measurements (Figure 4). Figure 4 summarizes the effects of δ^*, κ, and Re on the spatial-temporal movements of reattachment point (x_r^*) on the oscillating bottom wall, and separation ($x_s^* = x_s/H$) and reattachment ($x_{rs}^* = x_{rs}/H$) points on the stationary top wall with τ ($= \omega t$), as functions of δ^*, κ, and Re. The results indicate that (i) the spatial-temporal movements of x_r^*, x_s^*, and x_{rs}^* are strong functions of the imposed plate oscillations, (ii) x_r^* and x_s^* decrease during upward motion of the plate (i.e. the self-imposed adverse pressure gradient was reduced by the superimposed favourable gradient which then caused the reattachment and separation regions to move closer to the step), (iii) x_r^* and x_s^* increase during the downward motion, in which case an adverse pressure gradient was superimposed on the adverse pressure gradient due to the increase in ER, and caused x_r^* and x_s^* to move far downstream, and (iv) x_r^* and x_s^* are slightly out of phase with respect to each other.

4. CONCLUSIONS

The spatial-temporal movements of the reattachment and laminar separation points on the oscillating bottom and stationary top walls in a 2-D backward-facing step flow were characterized nonintrusively using multiple hot-film sensors arrays for

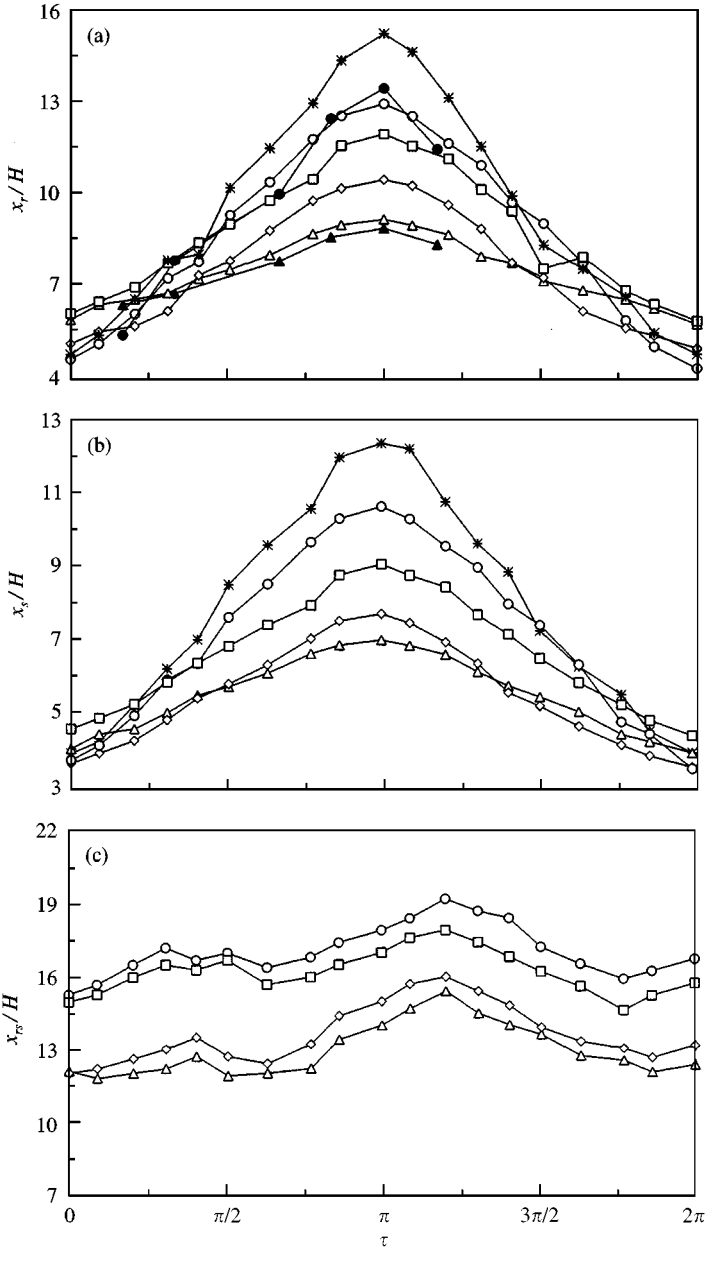

Figure 4. Variations of x_r^*, x_s^*, and x_{rs}^* with $\tau\,(=\omega t)$ as functions of δ^*, κ, and Re. (a) x_r^* on the oscillating bottom wall. (b)–(c) x_s^* and x_{rs}^* on the stationary top wall, respectively. Hot-film measurements: Δ, $\delta^* = \pm 0{\cdot}2$ and $\diamond$, $\delta^* = \pm 0{\cdot}33$ ($\kappa = 0{\cdot}08$ and Re = 535); $\square$, $\delta^* = \pm 0{\cdot}20$ and $\bigcirc$, $\delta^* = \pm 0{\cdot}60$ ($\kappa = 0{\cdot}04$ and Re = 745); *, $\delta^* = \pm 0{\cdot}41$ ($\kappa = 0{\cdot}08$ and Re = 1005). Smoke flow visualization results: $\bullet$, $\delta^* = \pm 0{\cdot}59$, $\kappa = 0{\cdot}04$, and Re = 745; $\blacktriangle$, $\delta^* = \pm 0{\cdot}22$, $\kappa = 0{\cdot}08$, and Re = 545.

Re < 1200. It is anticipated that the measurements are important in providing a practical means for the study of unsteady separated flows and an improved understanding of certain aspects of forced flow-induced vibrations, as well as in the validation of CFD predictions.

ACKNOWLEDGEMENTS

This work was supported by the NSERC of Canada and FCAR of the Province of Québec. Mr. J. Ghorayeb is thanked for his help with the design and fabrication of the flow facility.

References

Abbott, D. E. & Kline, S. J. 1962 Experimental investigations of subsonic turbulent flow over single and double backward-facing steps. *ASME Journal of Basic Engineering* **84,** 317–325.

Armaly, B. F., Durst, F., Pereira, J. C. F. & Schonung, B. 1983 Experimental and theoretical investigation of backward-facing step flow. *Journal of Fluid Mechanics* **127,** 473–496.

Driver, D. M., Seegmiller, H. L. & Marvin, J. G. 1987 Time-dependent behavior of a reattaching shear layer. *AIAA Journal* **25,** 914–919.

Eaton, J. K., Jeans, A. H., Ashjaee, J. & Johnston, J. P. 1979 A wall-flow-direction probe for use in separating and reattaching flows. *ASME Journal of Fluids Engineering* **101,** 364–366.

Eaton, J. K. & Johnston, J. P. 1981 A review of research on subsonic turbulent flow reattachment. *AIAA Journal* **19,** 1093–1100.

Gartling, D. K. 1990 A test problem for outflow boundary conditions—flow over a backward-facing step. *International Journal of Numerical Methods in Fluids* **11**, 953–967.

Goldstein, R. J., Eriksen, V. L., Olson, R. M. & Eckert, E. R. G. 1970 Laminar separation, reattachment and transition of the flow over a downstream-facing step. *ASME Journal of Basic Engineering* **92,** 732–741.

Grant, I., Owens, E., Yan, Y.-Y. & Shen, X. 1992 Particle image velocimetry measurements of the separated flow behind a rearward facing step. *Experiments in Fluids* **12,** 238–244.

Lee, T. & Mateescu, D. 1998 Experimental and numerical investigation of 2-D backward-facing flow. *Journal of Fluids and Structures* **12,** 703–716.

Lee, T., & Basu, S. 1998 Measurement of unsteady boundary layer developed on an oscillating airfoil using multiple hot-film sensors. *Experiments in Fluids* **25,** 108–117.

Mateescu, D., Païdoussis, M. P. & Bélanger, F. 1994 A time-integration method using artificial compressibility for unsteady viscous flows. *Journal of Sound and Vibration* **177,** 197–205.

Mullin, T., Greated, C. A. & Grant, I. 1980 Pulsating flow over a step. *Physics of Fluids* **23,** 669–674.

Westphal, R. V. & Johnston, J. P. 1984 Effect of initial conditions on turbulent reattachment downstream of a backward-facing step. *AIAA Journal* **22,** 1727–1731.